Supplement of Geosci. Model Dev., 17, 1327–1347, 2024
https://doi.org/10.5194/gmd-17-1327-2024-supplement

Geoscientific Model Development
Open Access
EGU

Supplement of

Assessing the sensitivity of aerosol mass budget and effective radiative forcing to horizontal grid spacing in E3SMv1 using a regional refinement approach

Jianfeng Li et al.

Correspondence to: Jianfeng Li (jianfeng.li@pnnl.gov) and Kai Zhang (kai.zhang@pnnl.gov)

Table S1. Evaluation statistics of aerosol optical depth (AOD) at 550 nm based on Figure S1

	MODIS[1]	LR			RRM		
	Mean[2]	Mean	RMSE	r	Mean	RMSE	r
ANN	0.159	0.130	0.084	0.66	0.130	0.084	0.66
JJA	0.164	0.149	0.098	0.72	0.149	0.099	0.72
DJF	0.162	0.130	0.092	0.68	0.129	0.093	0.68

[1]We use the level-3 MODIS (Moderate Resolution Imaging Spectroradiometer) gridded (1° × 1°) monthly Dark Target AOD products (MOD08_M3 and MYD08_M3) in 2016 (Platnick et al., 2015). MOD08_M3 provides monthly mean AOD at 10:30 local solar time (LST), while MYD08_M3 provides monthly mean AOD at 13:30 LST. The averages of monthly MOD08_M3 and MYD08_M3 AOD are used to calculate the MODIS annual, JJA (June, July, and August), and DJF (December, January, and February) mean AOD all over the globe in Figure S1, which are then used to derive the statistics here.

[2]"Mean" refers to the global mean; RMSE (root-mean-square-error) and r (Pearson correlation coefficient) are against MODIS observations.

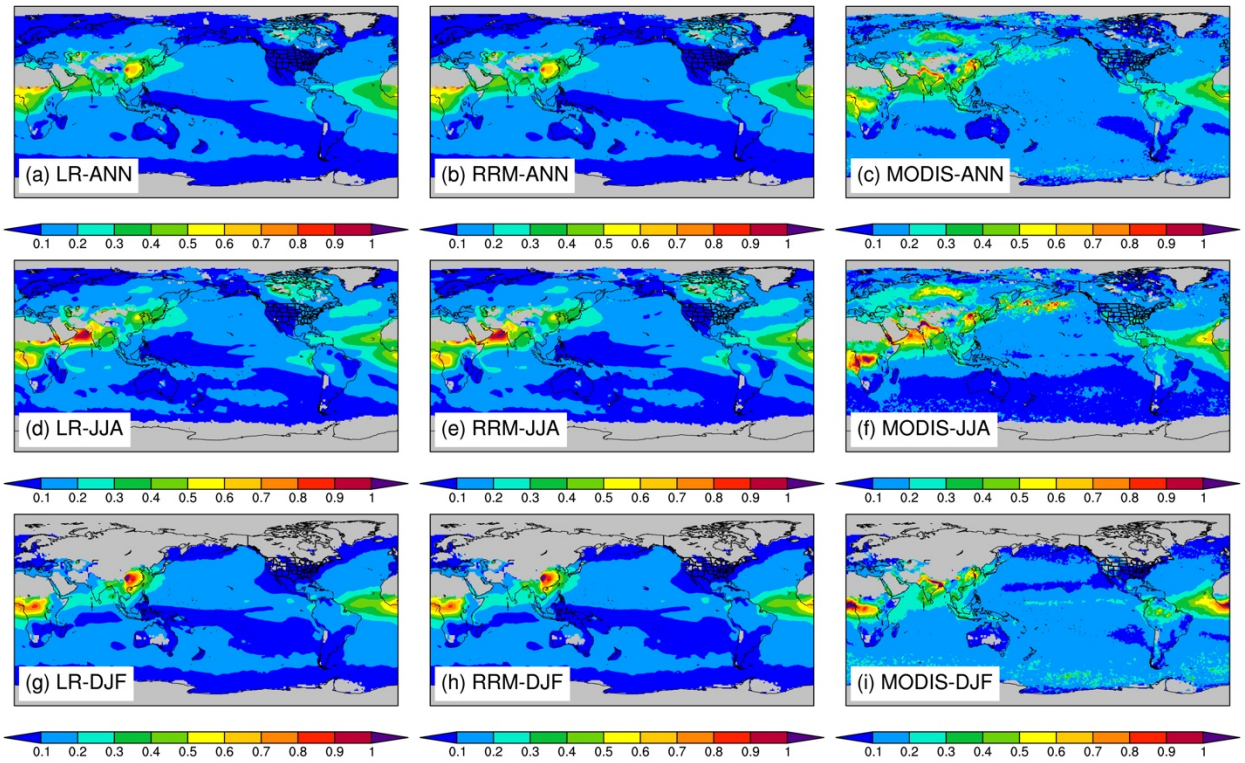

Figure S1. Spatial distributions of AOD at 550 nm from the (a, d, g) LR and (b, e, h) RRM simulations and (c, f, i) the MODIS datasets in 2016. (a, b, c) ANN refers to the annual mean, (d, e, f) JJA indicates the mean AOD during June, July, and August, and (g, h, i) represents the mean during December, January, and February. For the LR and RRM simulations, we output averaged AOD during 10:00-11:00 LST and 13:00-14:00 LST each day to match MOD and MYD observations, respectively. Calculated monthly AOD during the two periods from the LR and RRM simulations are then filtered using the corresponding data availability of MOD08_M3 and MYD08_M3 AOD at 550 nm, which are then used to calculate averaged AOD of the two periods). Finally, we use the monthly averaged AOD to calculate the annual, JJA, and DJF mean AOD for the LR and RRM simulations and the MODIS datasets.

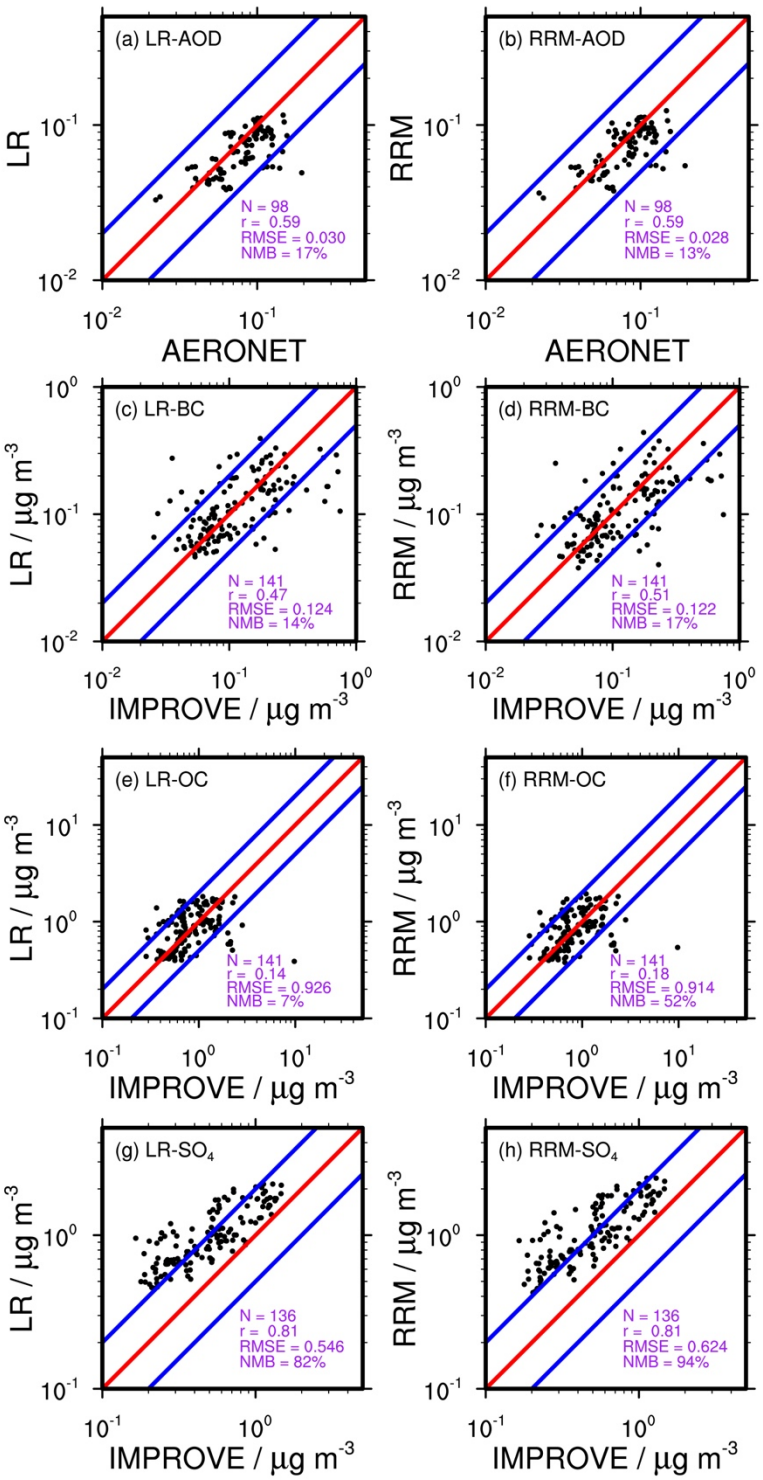

Figure S2. Evaluations of the (left column) LR and (right column) RRM simulated annual mean (a, b) AOD at 550 nm and fine (c, d) BC, (e, f) organic carbon (OC), and (g, h) SO_4 mass concentrations against ground-based observations from AERONET (AErosol RObotic NETwork) and IMPROVE (Interagency Monitoring of Protected Visual Environments) (Malm et al., 1994) in the RRM region in 2016. AERONET V3 level 2.0 provides daily mean AOD at 500 nm and daily mean Angstrom exponent for 440-870 nm (Slutsker, 2018), which are used to derive daily mean AOD at 550 nm. IMPROVE provides daily mean mass concentrations of fine BC, OC, and SO_4 (Cira/Csu, 2023). The daily mean observations

are used to calculate monthly means, which are then used to select coincident model monthly results. Notably, we use the regridded (1°× 1°) LR and RRM simulation results to match observational sites to make the comparisons fair to both simulations. Each dot in the figure denotes one observational site. "N" refers to the number of observational sites; "r" is the Pearson correlation coefficient; "RMSE" is the root mean square error; and "NMB" indicates the normalized mean bias.

We apply the following equations to calculate the model fine BC, OC, and SO_4 to be compared with observations.

SO_4(fine) = SO_4(accumulation mode) + SO_4(Aitken mode) + Sea salt(accumulation) + Sea salt(Aitken)

OC(fine) = (POM(primary carbon) + POM(accumulation) + SOA(accumulation) + SOA(Aitken))/1.4

BC(fine) = BC(accumulation) + BC(primary carbon)

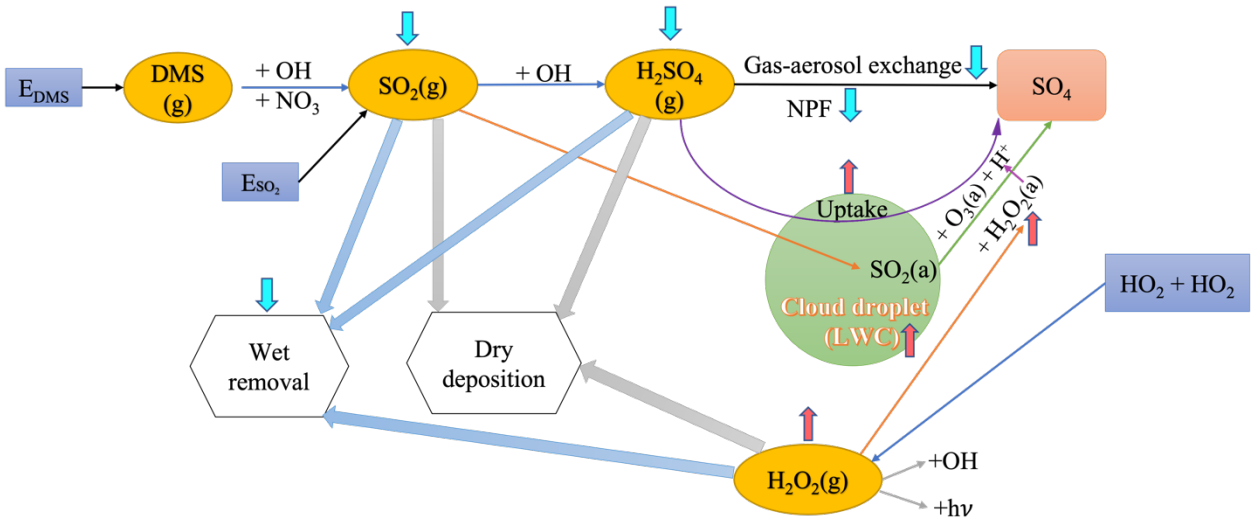

Figure S3. Schematic of the impact of RRM on sulfur chemistry. Red upward arrows indicate enhancement by RRM, while cyan downward arrows denote reduction by RRM.

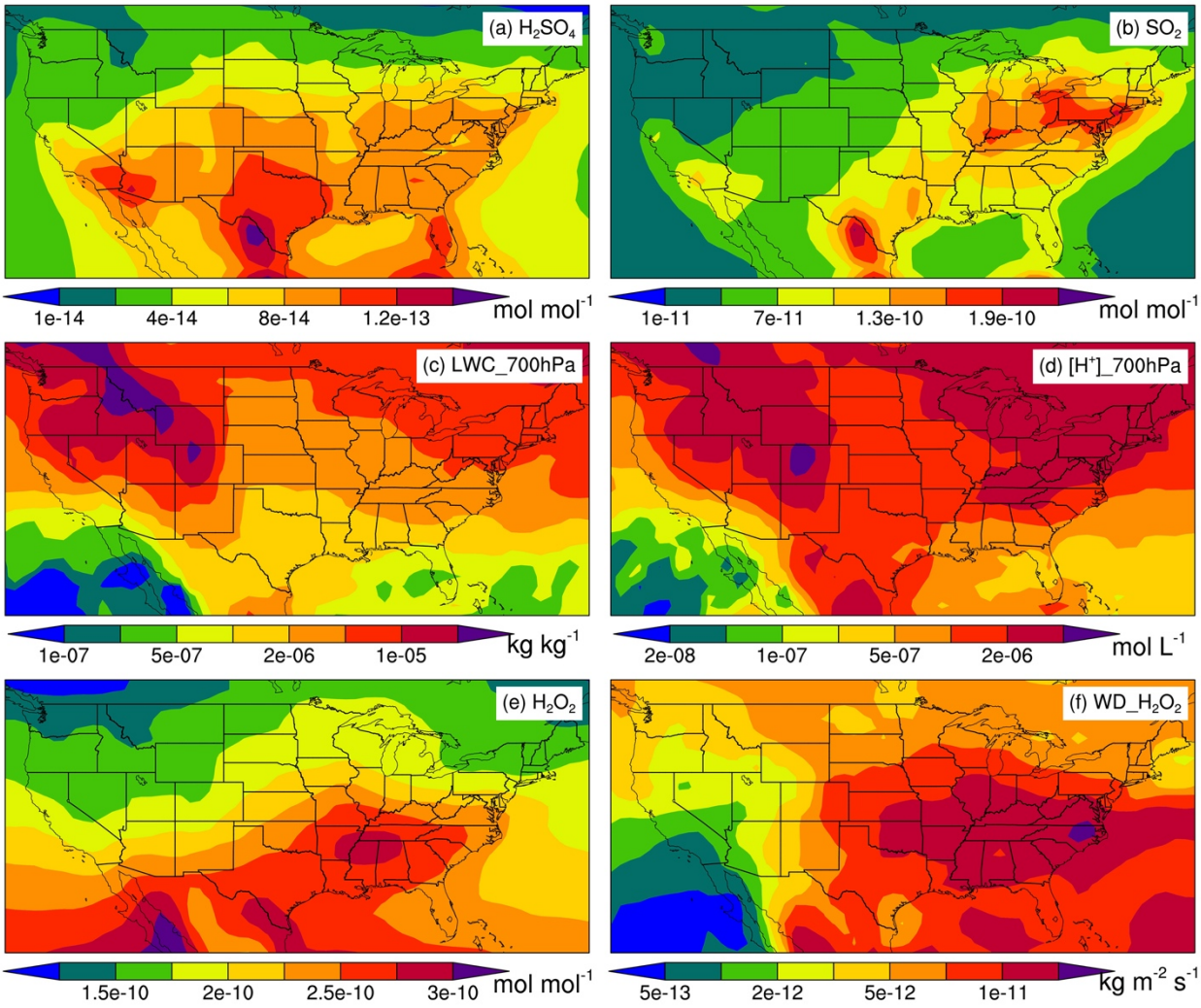

Figure S4. Spatial distributions of the annual mean (a) vertical-integrated gas-phase H_2SO_4 concentrations, (b) vertical-integrated gas-phase SO_2 concentrations, (c) large-scale cloud liquid water content at 700 hPa (kg_{water} kg_{air}^{-1}), (d) H^+ concentrations in large-scale cloud liquid water at 700 hPa, (e) vertical-integrated gas-phase H_2O_2 concentrations, and (f) wet deposition fluxes of gas-phase H_2O_2 from the LR simulation.

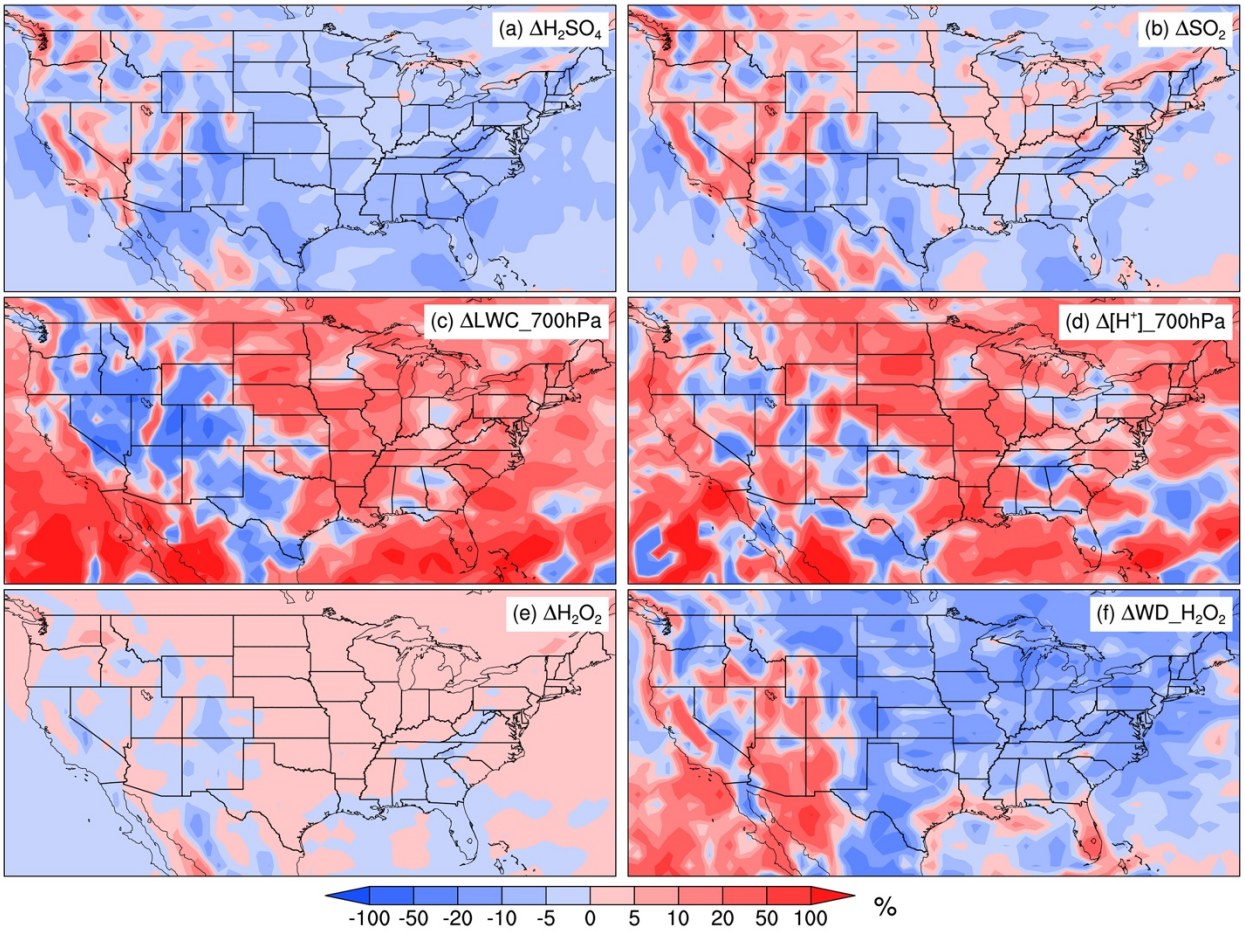

Figure S5. The same as Figure S2 but for the relative differences between the RRM and LR simulations.

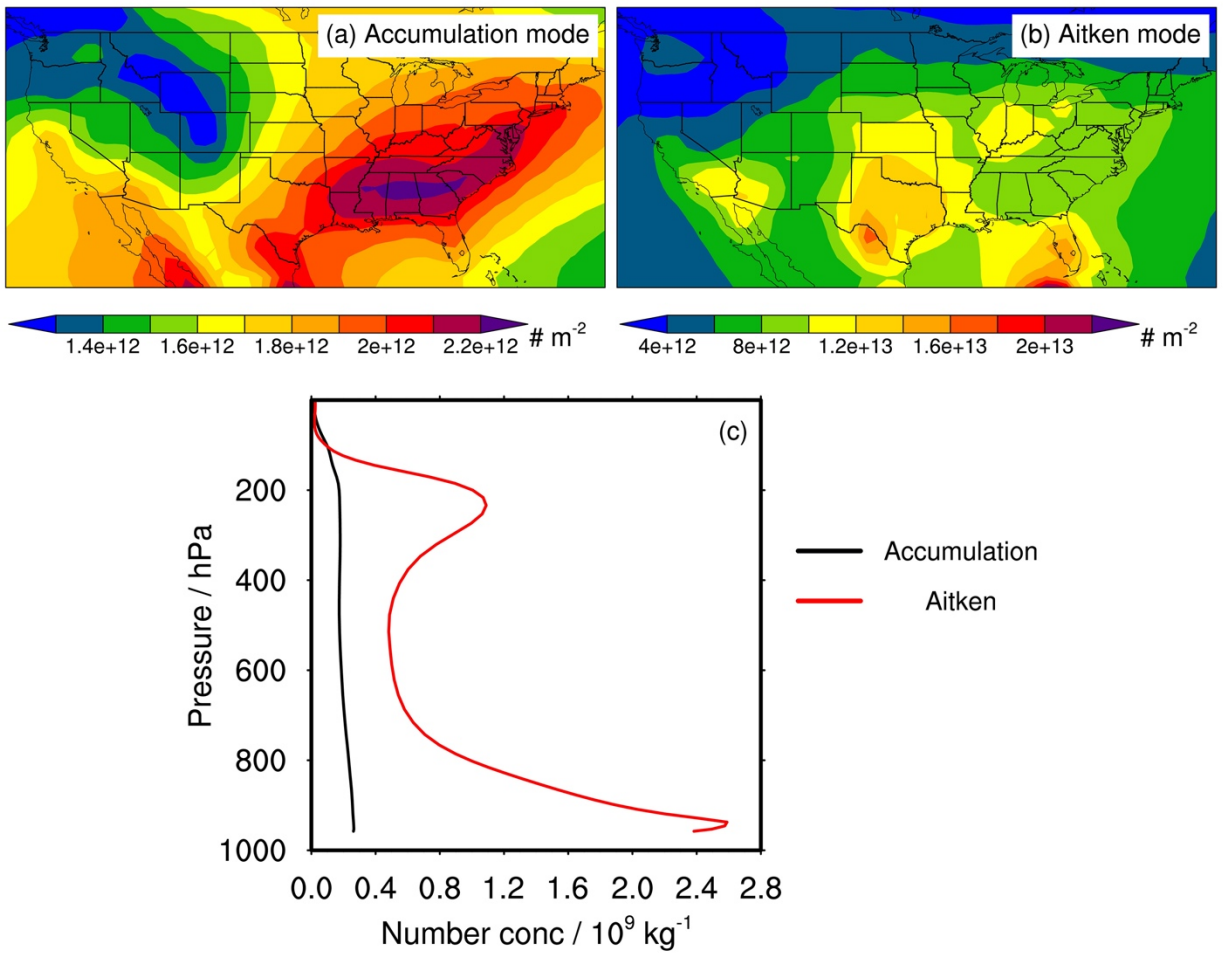

Figure S6. (a, b) Spatial distributions of annual mean vertical-integrated IAP number concentrations (# m^{-2}) for (a) accumulation and (b) Aitken modes from the LR simulation. (c) Vertical profiles of annual regional mean IAP number concentrations (10^9 kg_{air}^{-1}) for accumulation and Aitken modes from the LR simulation.

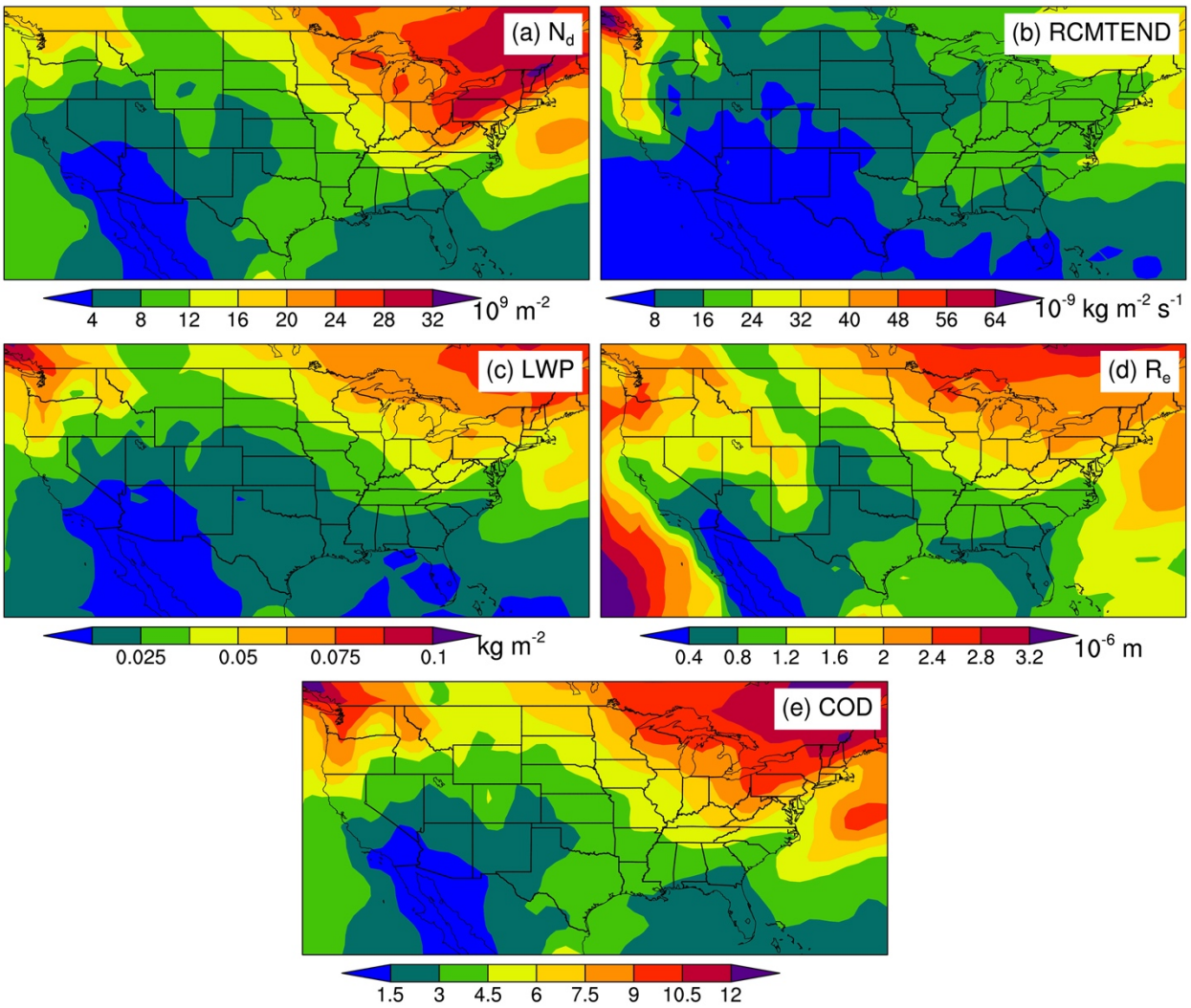

Figure S7. Same as Figure 12 but for the LR simulation results.

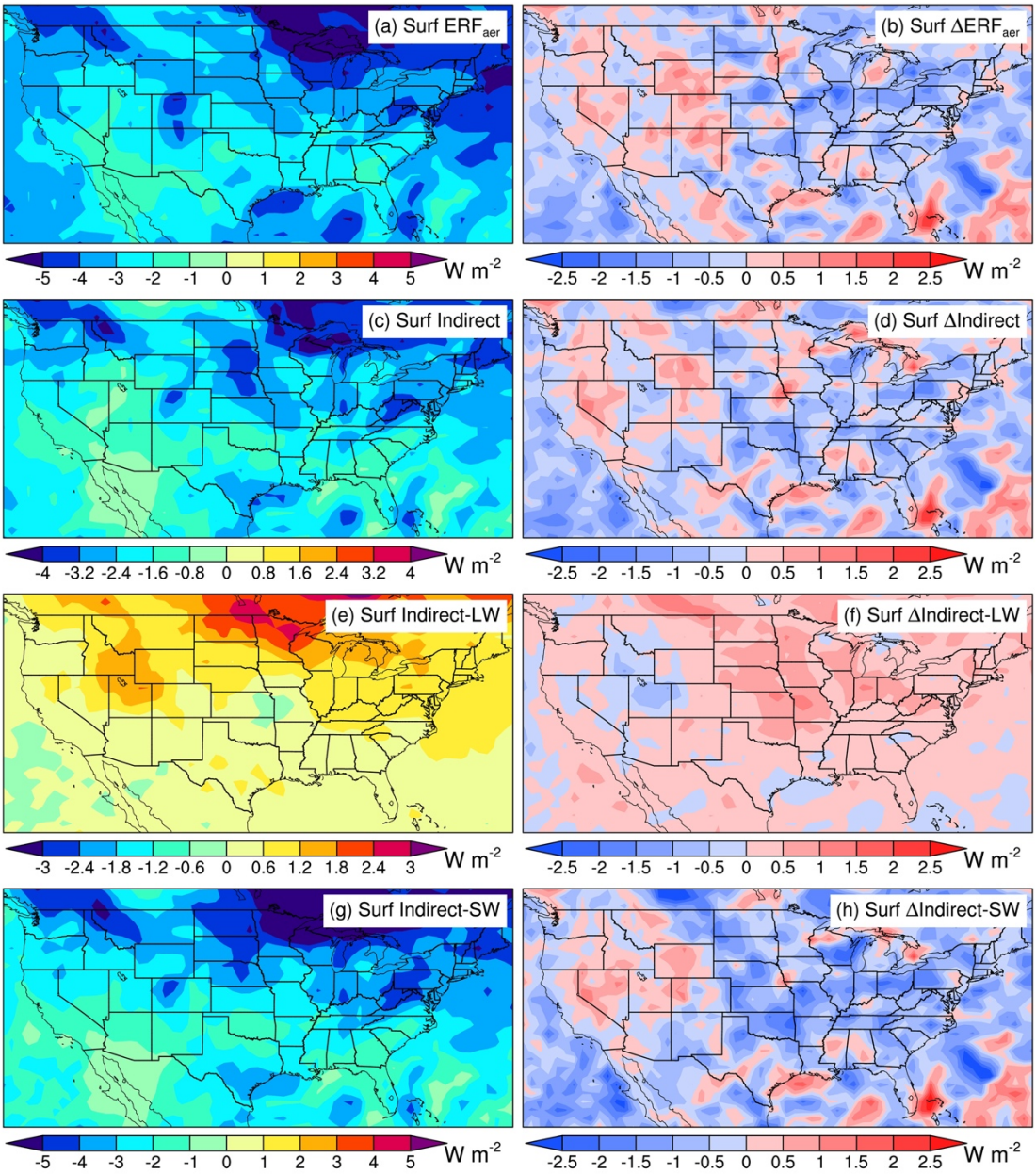

Figure S8. Same as Figure 13 but for surface ERF$_{aer}$.

References

CIRA/CSU: IMPROVE Data, Federal Land Manager Environmental Database [dataset], https://views.cira.colostate.edu/fed/QueryWizard/, 2023 (last access: May 26, 2022).

Malm, W. C., Sisler, J. F., Huffman, D., Eldred, R. A., and Cahill, T. A.: Spatial and seasonal trends in particle concentration and optical extinction in the United States, Journal of Geophysical Research: Atmospheres, 99, 1347-1370, https://doi.org/10.1029/93JD02916, 1994.

Platnick, S., King, M., and Hubanks, P.: MODIS Atmosphere L3 Monthly Product, NASA MODIS Adaptive Processing System, Goddard Space Flight Center [dataset], https://doi.org/10.5067/MODIS/MOD08_M3.061 (MOD08_M3) and https://doi.org/10.5067/MODIS/MYD08_M3.061 (MYD08_M3), 2015 (last access: Nov 28, 2023).

Slutsker, I.: Aerosol Robotic Network, Goddard Space Flight Center [dataset], https://aeronet.gsfc.nasa.gov/new_web/download_all_v3_aod.html, 2018 (last access: May 26, 2022).